PROCEEDINGS OF SCIENCE

Status and prospects of rare decay searches at LHCb

Gabriele Martelli[a,*] **on behalf of the LHCb collaboration**

[a] *University of Perugia and INFN Perugia,*
Via Alessandro Pascoli 23c, Perugia, Italy

E-mail: gabriele.martelli@cern.ch, gabriele.martelli@pg.infn.it

This contribution presents the latest results on rare and very rare decays from the LHCb experiment. These results include amplitude measurements in B decays, tests of lepton flavour universality, and studies of charm and strange decays.

Workshop Italiano sulla Fisica ad Alta Intensità (WIFAI 2024)
12-15 November 2024
Bologna, Italy

*Speaker

© Copyright owned by the author(s) under the terms of the Creative Commons Attribution-NonCommercial-NoDerivatives 4.0 International License (CC BY-NC-ND 4.0).
All rights for text and data mining, AI training, and similar technologies for commercial purposes, are reserved.
ISSN 1824-8039. Published by SISSA Medialab.

PoS(WIFAI2024)016

1. Introduction

Despite its remarkable successes, the Standard Model (SM) remains an incomplete framework, leaving several fundamental questions unanswered. Exploring the flavour sector, delving into the properties and interactions of different particle flavours and the mixing between them, can help study many of its problems. The Large Hadron Collider beauty (LHCb) experiment at CERN has established itself as an ideal setting for investigating flavour physics.

The LHCb detector [1][2] is a single-arm forward spectrometer covering the pseudorapidity range $2 < \eta < 5$, designed for the study of particles containing b or c quarks. Within LHCb, the rare and very rare decay search programs continue to push the understanding of particle physics by shedding light on the most elusive and intriguing processes involving hadrons.

The next sections present new LHCb results on amplitude analyses of the $B_s^0 \to K^+K^-\gamma$ and $B^0 \to K^{*0}\mu^+\mu^-$ decays. These are followed by tests of lepton flavour universality using the $B_s^0 \to \phi\ell^+\ell^-$ and $B^+ \to K^+\pi^+\pi^-\ell^+\ell^-$ processes, as well as studies on the $\Lambda_c^+ \to p\mu^+\mu^-$ and $\Sigma^+ \to p\mu^+\mu^-$ decays.

The inclusion of charge-conjugated processes is implied throughout this contribution.

2. Amplitude analysis of the radiative decay $B_s^0 \to K^+K^-\gamma$

A search for radiative decays of B_s^0 mesons to orbitally excited K^+K^- states is reported. The results are obtained using proton-proton (pp) collision data collected at a centre-of-mass energy of 7, 8 and 13 TeV, corresponding to an integrated luminosity of 9 fb^{-1} [3]. This is the first amplitude analysis of the dikaon resonant structure in the $B_s^0 \to K^+K^-\gamma$ decay up to a dikaon invariant mass of $m_{KK} = 2400$ MeV/c^2.

The amplitude fit is simplified by three key features: the absence of an S-wave component, the cancellation of the interference of odd and even spin resonance and the cancellation of detector asymmetries by folding the helicity angle observable by the operation $\cos\theta_{KK} \to |\cos\theta_{KK}|$.

The signal amplitudes are fitted in the $(m_{KK}, |\cos\theta_{KK}|)$ plane using an isobar model. Considering the possible contributions of $f_2(1270)$, $f_2'(1525)$ and $f_2(2010)$ meson states, the overall tensor contribution to the amplitude is measured to be

$$\mathcal{F}_{\{f_2\}} = 16.8 \pm 0.5\ (\text{stat}) \pm 0.7(\text{sys})\%. \tag{1}$$

Different statistically equivalent solutions are obtained for the detailed resonant structure, depending on whether the smaller amplitudes interfere constructively or destructively with the dominant one. The preferred one, which corresponds to the lowest values of the fit fractions and constructive interference, results in the measurement of the relative branching ratio

$$\frac{\mathcal{B}\left(B_s^0 \to f_2'\gamma\right)}{\mathcal{B}\left(B_s^0 \to \phi\gamma\right)} = 19.4^{+0.9}_{-0.8}(\text{stat.})^{+1.4}_{-0.5}(\text{syst.}) \pm 0.5(\text{ext.})\%, \tag{2}$$

where the last uncertainty is due to the ratio of measured branching fractions to the K^+K^- final state. This result represents the first observation of the radiative $B_s^0 \to f_2'(1525)\gamma$ decay, which is the second radiative transition observed in the B_s^0 sector.

PoS(WIFAI2024)016

3. Comprehensive analysis of local and nonlocal amplitudes in the $B^0 \to K^{*0}\mu^+\mu^-$ decay

LHCb performed a comprehensive study of the local and nonlocal amplitudes contributing to the $B^0 \to K^{*0}\mu^+\mu^-$ decay. The analysis is based on pp collision data recorded during the Run 1 and Run 2 periods, corresponding to an integrated luminosity of 8.4 fb^{-1} [4]. Previous LHCb measurements have investigated $B^0 \to K^{*0}\mu^+\mu^-$ decays with binned and unbinned methodologies using a dataset corresponding to an integrated luminosity of 4.7 fb^{-1} [5].

The decay rate of the $B^0 \to K^{*0}\mu^+\mu^-$ P-wave process is described by transversity amplitudes that depend on the Wilson Coefficients (WCs) and $B \to K^*$ form factors. The nonlocal model, which includes all vector resonances that couple to muons and contributions from $D^{(*)}\bar{D}^{(*)}$ and $\tau^+\tau^-$ loops, is

$$C_9^{\text{eff},\lambda}\left(q^2\right) = C_9^{\mu} + Y_{c\bar{c}}^{(0),\lambda} + Y_{c\bar{c}}^{1P,\lambda}\left(q^2\right) + Y_{\text{light}}^{1P,\lambda}\left(q^2\right) + Y_{c\bar{c}}^{2P,\lambda}\left(q^2\right) + Y_{\tau\bar{\tau}}\left(q^2\right). \tag{3}$$

An angular analysis is performed using three decay angles $\Omega = (\cos\theta_K, \cos\theta_\ell, \phi)$ and q^2. The fit to the data leads to the following WCs

$$\begin{aligned} C_9 &= 3.56 \pm 0.28 \pm 0.18 \\ C_{10} &= -4.02 \pm 0.18 \pm 0.16 \\ C_9' &= 0.28 \pm 0.41 \pm 0.12 \\ C_{10}' &= -0.09 \pm 0.21 \pm 0.06 \\ C_{9\tau} &= -(1.0 \pm 2.6 \pm 1.0) \times 10^2 \end{aligned} \tag{4}$$

C_9 exhibits a 2.1σ deviation from the SM expectation while C_{10}, C_9' and C_{10}' are all in better agreement with the SM, with a global significance at the level of 1.5σ. The resulting angular observable P_5', constructed out of the signal parameters from the baseline ft to data, is shown in Fig. 1. This measurement indicates that the non-local contribution, if embedded in the decay amplitude model accounting for different sources as in Eq .3, is not sufficient to explain the deviations in the measured value of C_9.

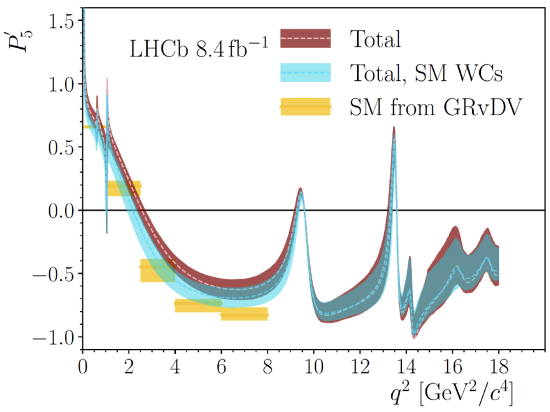

Figure 1: The P_5' angular observable as a function of q^2 obtained from the fit to data (red), compared to SM model predictions (yellow) and the fit result with the WC set to the SM values (cyan).

PoS(WIFAI2024)016

4. Test of lepton flavour universality with $B_s^0 \to \phi\ell^+\ell^-$ decays

A first measurement of the lepton universality ratio R_ϕ is reported, using pp collision data collected at a centre-of-mass energy of 7, 8 and 13 TeV, corresponding to an integrated luminosity of 9 fb^{-1} [6].

The analysis is performed in three regions of q^2: $0.1 < q^2 < 1.1$ (low), $1.1 < q^2 < 6.0$ (central) and $15 < q^2 < 19$ (high) GeV$^2/c^4$. The double ratio of branching fractions is measured as [7] [8]

$$R_\phi = \left(\frac{\mathcal{B}\left(B_s^0 \to \phi\mu^+\mu^-\right)}{\mathcal{B}\left(B_s^0 \to J/\psi\,(\to \mu^+\mu^-)\,\phi\right)} \right) / \left(\frac{\mathcal{B}\left(B_s^0 \to \phi e^+e^-\right)}{\mathcal{B}\left(B_s^0 \to J/\psi\,(\to e^+e^-)\,\phi\right)} \right). \tag{5}$$

R_ϕ^{-1} is measured rather than R_ϕ so that the small $B_s^0 \to \phi e^+e^-$ yield appears in the numerator and the statistical behaviour of the observable more closely follows a Gaussian distribution.

Results on R_ϕ^{-1} in the three q^2 regions are shown in Tab. 1 while the variation with R_ϕ^{-1} of the difference in log-likelihood of the fit from the best-fit point is illustrated in Fig. 2. The values confirm a good agreement with the SM prediction.

Table 1: Values of R_ϕ^{-1} and $\mathrm{d}\mathcal{B}\left(B_s^0 \to \phi e^+e^-\right)/\mathrm{d}q^2$ in the low-, central- and high-q^2 regions. The first uncertainty is statistical and the second systematic. For the differential branching fraction, the third and the fourth uncertainties are due to the experimental uncertainty on the ratio $\mathrm{d}\mathcal{B}\left(B_s^0 \to \phi\mu^+\mu^-\right)/\mathrm{d}q^2/\mathcal{B}\left(B_s^0 \to J/\psi\phi\right)$ and on $\mathcal{B}\left(B_s^0 \to J/\psi\phi\right)$, respectively.

q^2 [GeV$^2/c^4$]	R_ϕ^{-1}	$\mathrm{d}\mathcal{B}\left(B_s^0 \to \phi e^+e^-\right)/\mathrm{d}q^2$ [10^{-7}GeV$^{-2}c^4$]
$0.1 < q^2 < 1.1$	$1.57^{+0.28}_{-0.25} \pm 0.05$	$1.38^{+0.25}_{-0.22} \pm 0.04 \pm 0.19 \pm 0.06$
$1.1 < q^2 < 6.0$	$0.91^{+0.20}_{-0.19} \pm 0.05$	$0.26 \pm 0.06 \pm 0.01 \pm 0.01 \pm 0.01$
$15.0 < q^2 < 19.0$	$0.85^{+0.24}_{-0.23} \pm 0.10$	$0.39 \pm 0.11 \pm 0.04 \pm 0.02 \pm 0.02$

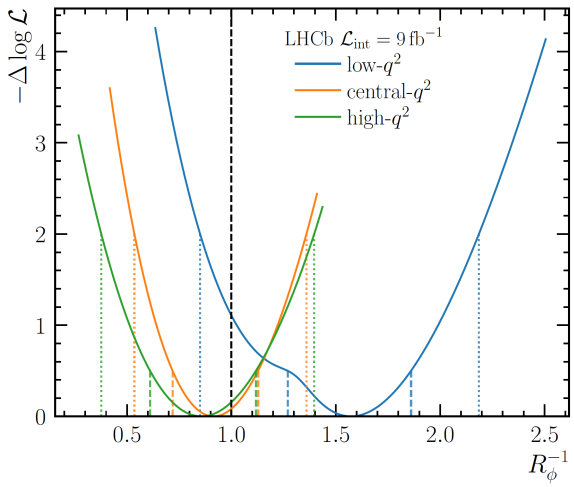

Figure 2: Profile log-likelihood of R_ϕ^{-1} for the low-, central- and high-q2 bins, relative to the best fit point. The vertical lines indicate the 1 and 2 σ confidence intervals, respectively.

PoS(WIFAI2024)016

5. Test of lepton flavour universality with $B^+ \to K^+\pi^+\pi^-\ell^+\ell^-$ decays

The first test of lepton flavour universality between muons and electrons using $B^+ \to K^+\pi^+\pi^-\ell^+\ell^-$ ($\ell = e, \mu$) decays is presented. The measurement is performed with pp collision data collected at a centre-of-mass energy of 7, 8 and 13 TeV, corresponding to an integrated luminosity of 9 fb^{-1} [9].

The measured observable is chosen to be $R^{-1}_{K\pi\pi}$, defined as a double ratio by normalising the signal-mode branching fractions to those of the corresponding $J\psi$ control mode,

$$R^{-1}_{K\pi\pi} \equiv \frac{\frac{\mathcal{N}}{\varepsilon}\left(B^+ \to K^+\pi^+\pi^- e^+e^-\right)}{\frac{\mathcal{N}}{\varepsilon}\left[B^+ \to K^+\pi^+\pi^- J/\psi\,(\to e^+e^-)\right]} \Big/ \frac{\frac{\mathcal{N}}{\varepsilon}\left(B^+ \to K^+\pi^+\pi^-\mu^+\mu^-\right)}{\frac{\mathcal{N}}{\varepsilon}\left[B^+ \to K^+\pi^+\pi^- J/\psi\,(\to \mu^+\mu^-)\right]}, \tag{6}$$

where $\frac{\mathcal{N}}{\varepsilon}$ are the efficiency-corrected yields.

$R^{-1}_{K\pi\pi}$ is determined from a simultaneous fit to the invariant mass spectra of signal $B^+ \to K^+\pi^+\pi^-\ell^+\ell^-$ and $B^+ \to K^+\pi^+\pi^- J/\psi\,(\to \ell^+\ell^-)$ decays, as illustrated in Fig. 3.

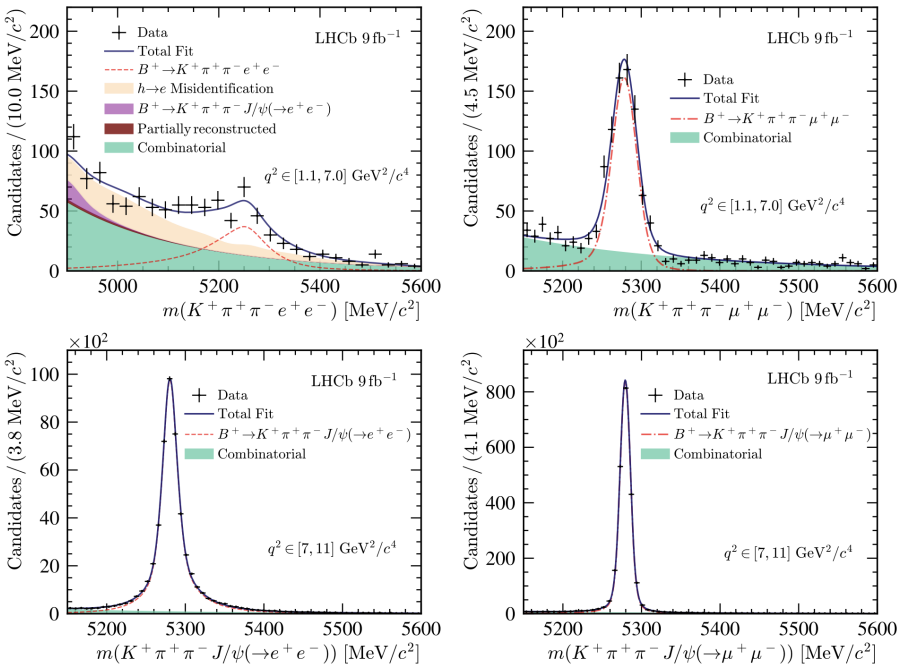

Figure 3: Invariant mass distributions together with the fit results of (top left) signal $B^+ \to K^+\pi^+\pi^- e^+e^-$, (top right) signal $B^+ \to K^+\pi^+\pi^-\mu^+\mu^-$, (bottom left) control $B^+ \to K^+\pi^+\pi^- J/\psi\,(\to e^+e^-)$ and (bottom right) control $B^+ \to K^+\pi^+\pi^- J/\psi\,(\to \mu^+\mu^-)$ decays, where the shaded background components are stacked.

The measured signal yields are $\mathcal{N}\left(B^+ \to K^+\pi^+\pi^- e^+e^-\right) = 264 \pm 21$ and $\mathcal{N}\left(B^+ \to K^+\pi^+\pi^-\mu^+\mu^-\right) = 731 \pm 31$, where the uncertainties only include the statistical component. The $R^{-1}_{K\pi\pi}$ observable is measured to be

$$R^{-1}_{K\pi\pi} = 1.31^{+0.18}_{-0.17}(\text{stat})^{+0.12}_{-0.09}\,(\text{syst})\,, \tag{7}$$

where the first set of uncertainties are statistical and the second systematic. The result is in agreement with the SM expectation of LFU at the level of 1.7 standard deviations.

PoS(WIFAI2024)016

6. Search for the rare decay of charmed baryon Λ_c^+ into the $p\mu^+\mu^-$ final state

A search for the non-resonant $\Lambda_c^+ \to p\mu^+\mu^-$ decay is performed using pp collision data recorded at a center-of-mass energy of 13 TeV, corresponding to an integrated luminosity of 5.4 fb^{-1} [10].

The analysis is carried out in six different regions of dimuon invariant mass $m_{\mu\mu}$, as reported in Tab. 2. The non-resonant signal decay is searched for in two $m_{\mu\mu}$ regions, low-m and high-m, where the expected contributions of resonances are subdominant. In the following, the combination of these two ranges is referred to as the signal region. The non signal range is divided into regions where either the η, ρ, ω or ϕ resonance dominates.

Table 2: Definitions of the dimuon invariant-mass ranges. The lower (upper) bound of the low-m (high-m) region corresponds to the phase-space limits.

Region	Range $\left[\text{MeV}/c^2\right]$
low-m	$211.32 < m_{\mu^+\mu^-} < 507.86$
high-m	$1059.46 < m_{\mu^+\mu^-} < 1348.13$
η	$507.86 < m_{\mu^+\mu^-} < 587.86$
ω	$742.65 < m_{\mu^+\mu^-} < 822.65$
ρ	$587.86 < m_{\mu^+\mu^-} < 742.65$
	or $822.65 < m_{\mu^+\mu^-} < 965.20$
ϕ	$979.46 < m_{\mu^+\mu^-} < 1059.46$

An unbinned fit is performed to the $m_{p\mu\mu}$ invariant mass in regions of the dimuon mass. No amplitude analysis is performed, hence interferences between resonances or with the non-resonant part are not considered.

Significant signals are obtained in the ρ, ω and ϕ regions. An evidence of 3 standard deviations is also obtained in the η region. The corresponding branching fractions are estimated using the $\Lambda_c^+ \to p\phi\,(\to \mu^+\mu^-)$ as normalisation channnel, having the same final state as the signal and being relatively abundant. The corresponding branching fractions are determined to be

$$\begin{aligned}
\mathcal{B}\left(\Lambda_c^+ \to p\omega\right) &= (9.82 \pm 1.23\ (\text{stat.}) \ \pm 0.73\ (\text{syst.}) \ \pm 2.79\ (\text{ext.})\ ) \times 10^{-4} \\
\mathcal{B}\left(\Lambda_c^+ \to p\rho\right) &= (1.52 \pm 0.34\ (\text{stat.}) \ \pm 0.14\ (\text{syst.}) \ \pm 0.24\ (\text{ext.})\ ) \times 10^{-3} \\
\mathcal{B}\left(\Lambda_c^+ \to p\eta\right) &= (1.67 \pm 0.69\ (\text{stat.}) \ \pm 0.23\ (\text{syst.}) \ \pm 0.34\ (\text{ext.})\ ) \times 10^{-3}.
\end{aligned} \tag{8}$$

No evidence for Λ_c^+ into the $p\mu^+\mu^-$ decays is instead obtained in the non-resonant regions, and an upper limit for a non-resonant Λ_c^+ into the $p\mu^+\mu^-$ is estimated

$$\frac{\mathcal{B}\left(\Lambda_c^+ \to p\mu^+\mu^-\right)}{\mathcal{B}\left(\Lambda_c^+ \to p\phi\right)\mathcal{B}\left(\phi \to \mu^+\mu^-\right)} < 0.09(0.10) \text{ at } 90\%\ (95\%)\ \text{CL}. \tag{9}$$

Using the branching fractions values of the $\Lambda_c^+ \to p\phi$ and $\phi \to \mu^+\mu^-$ decays, the result leads to $\mathcal{B}\left(\Lambda_c^+ \to p\mu^+\mu^-\right) < 2.9(3.2) \times 10^{-8}$ at 90%(95%)CL, which is the most stringent limit to date.

PoS(WIFAI2024)016

7. Observation of the $\Sigma^+ \to p\mu^+\mu^-$ decay ay LHCb

The first observation of the $\Sigma^+ \to p\mu^+\mu^-$ decay is reported with high significance using pp collision data, corresponding to an integrated luminosity of 5.4 fb^{-1}, collected at a centre-of-mass energy of 13 TeV. Furthermore, no significant structure is observed in the dimuon invariant mass distribution, which is compatible with SM expectations [11].

Evidence for the decay was reported by the HyperCP experiment with the observation of three background-free events, corresponding to a branching fraction of $\mathcal{B}(\Sigma^+ \to p\mu^+\mu^-) = \left(8.6^{+6.6}_{-5.4} \pm 5.5\right) \cdot 10^{-8}$, compatible with the SM predictions [12]. The three events had the same values of dimuon invariant mass, pointing towards a $\Sigma^+ \to pX^0\,(\to \mu^+\mu^-)$ decay, with X^0 being a particle beyond the SM with a mass $m_{X^0} = 214.3 \pm 0.5$ MeV/c^2. Many New Physics explanations were proposed for this possible particle and searches where conducted in different final states including a dimuon pair, without finding any evidence. A search for $\Sigma^+ \to p\mu^+\mu^-$ decays was performed at LHCb with Run 1 data [13], which produced evidence for this decay with about ten events and a branching fraction compatible with the SM. No structure in the dimuon mass was seen excluding the central value of the HyperCP branching fraction under the X^0 hypothesis.

With Run 2 data, a significantly improved trigger with dedicated lines for soft dimuons and rare strange decays was deployed, bringing to a factor 10 larger trigger efficiency. Furthermore, given the increased cross-section and integrated luminosity this brings almost two orders of magnitude of improvement. The signal yield is obtained, after full selection, with an unbinned fit to the $\Sigma^+ \to p\mu^+\mu^-$ mass, as shown in Fig. 4 (left). A clear peak is observed with very large significance and $N(\Sigma^+ \to p\mu^+\mu^-) = 279 \pm 19$ signal events are found. This constitutes the first observation of this channel, which is the rarest baryon decay ever observed. The dimuon invariant mass distribution is also examined in Fig. 4 (right). No evidence of any structure is present as the distribution is found very compatible with the SM prediction.

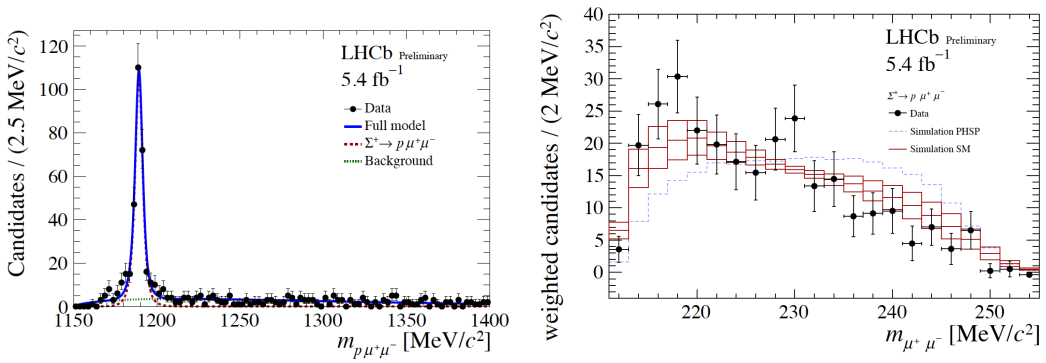

Figure 4: (Left) Distribution of the invariant mass of $\Sigma^+ \to p\mu^+\mu^-$ candidates with the result of an extended unbinned maximum likelihood fit superimposed (blue solid line). The signal (red dashed line) and background (green dotted line) components are also shown. (Right) Distribution of dimuon invariant mass for $\Sigma^+ \to p\mu^+\mu^-$ candidates in data compared with simulation. The LHCb phase space is shown weighted to follow the SM amplitude (red band) and without weights (blue line).

PoS(WIFAI2024)016

8. Conclusions

In summary, recent results on rare and very rare decays at LHCb are reported. Amplitude analyses of the $B_s^0 \to K^+K^-\gamma$ and $B^0 \to K^{*0}\mu^+\mu^-$ decays are illustrated. Additionally, tests of lepton flavour universality with $B_s^0 \to \phi\ell^+\ell^-$ and $B^+ \to K^+\pi^+\pi^-\ell^+\ell^-$ processes and studies on the $\Lambda_c^+ \to p\mu^+\mu^-$ and $\Sigma^+ \to p\mu^+\mu^-$ decays are presented.

References

[1] LHCb Collaboration, A. A. Alves Jr. *et al.*, *The LHCb detector at the LHC*, JINST **3** (2008) S08005, DOI:10.1088/1748-0221/3/08/S08005.

[2] LHCb Collaboration, R. Aaij *et al.*, *LHCb detector performance*, Int. J. Mod. Phys. **A30** (2015) 1530022, DOI:10.1142/S0217751X15300227, [arXiv:1412.6352 [hep-ex]].

[3] LHCb Collaboration, R. Aaij *et al.*, *Amplitude analysis of the radiative decay* $B_s^0 \to K^+K^-\gamma$, Journal of High Energy Physics **8** (2024) 93, DOI:10.1007/JHEP08(2024)093.

[4] LHCb Collaboration, R. Aaij *et al.*, *Comprehensive analysis of local and nonlocal amplitudes in the* $B^0 \to K^{*0}\mu^+\mu^-$ *decay*, Journal of High Energy Physics **9** (2024) 26, DOI:10.1007/JHEP09(2024)026.

[5] LHCb Collaboration, R. Aaij *et al.*, *Measurement of CP-Averaged Observables in the* $B^0 \to K^{*0}\mu^+\mu^-$ *decay*, Phys. Rev. Lett. **125** (2020) 011802, DOI:10.1103/PhysRevLett.125.011802.

[6] LHCb Collaboration, R. Aaij *et al.*, *Test of lepton flavour universality with* $B_s^0 \to \phi\ell^+\ell^-$ *decays*, **2410.13748** (2024), DOI:10.48550/arXiv.2410.13748.

[7] LHCb Collaboration, R. Aaij *et al.*, *Measurement of lepton universality parameters in* $B^+ \to K^+\ell^+\ell^-$ *and* $B^0 \to K^{*0}\ell^+\ell^-$ *decays*, Phys. Rev. **D108** (2023) 032002, DOI:10.1103/PhysRevD.108.032002.

[8] LHCb Collaboration, R. Aaij *et al.*, *Test of lepton universality in* $b \to s\ell^+\ell^-$ *decays*, Phys. Rev. Lett. **131** (2023) 051803, DOI:10.1103/PhysRevLett.131.051803.

[9] LHCb Collaboration, R. Aaij *et al.*, *Test of lepton flavour universality with* $B^+ \to K^+\pi^+\pi^-\ell^+\ell^-$ *decays*, **2412.11645** (2024), DOI:10.48550/arXiv.2412.11645.

[10] LHCb Collaboration, R. Aaij *et al.*, *Search for the rare decay of charmed baryon* Λ_c^+ *into the* $p\mu^+\mu^-$ *final state*, Phys. Rev. D **110** (2024) 052007, DOI:10.1103/PhysRevD.110.052007.

[11] LHCb Collaboration, R. Aaij *et al.*, *Observation of the* $\Sigma^+ \to p\mu^+\mu^-$ *decay at LHCb*, LHCb-CONF-2024-002.

[12] H. Park *et al.*, *Evidence for the decay* $\Sigma^+ \to p\mu^+\mu^-$, Phys. Rev. Lett. **94** (2005) 021801, DOI:10.1103/PhysRevLett.94.021801.

[13] LHCb Collaboration, R. Aaij *et al.*, *Evidence for the rare decay* $\Sigma^+ \to p\mu^+\mu^-$, Phys. Rev. Lett. **120** (2018) 221803, DOI:10.1103/PhysRevLett.120.221803.

PoS(WIFAI2024)016